Burnt areas semantic segmentation from Sentinel data using the U-Net network trained with semi-automated annotations

BURNT AREAS SEMANTIC SEGMENTATION FROM SENTINEL DATA USING THE U-NET NETWORK TRAINED WITH SEMI-AUTOMATED ANNOTATIONS

A. B. Marra [1], M. L. B. T. Galo [1], F. Giulio Tonolo [2], E. E. Sano[3], V. S. W. Orlando [1]

[1] São Paulo State University (UNESP), Presidente Prudente, São Paulo, Brazil - (aline.barroca, trindade.galo, vinicius.werneck)@unesp.br
[2] Politecnico di Torino, Dept. of Architecture and Design, Turin, Italy - fabio.giuliotonolo@polito.it
[3] Embrapa Cerrados, Planaltina, Distrito Federal, Brazil - edson.sano@embrapa.br

KEY WORDS: Burnt area detection, U-Net, Semantic segmentation, Copernicus Sentinels, Semi-automatic annotation, Brazilian Pantanal.

ABSTRACT:

The Pantanal biome is one of the most important wetlands on the planet, harboring a rich biodiversity whilst being critical in maintaining hydrological cycles and climate regulation. However, the occurrence of fires in the biome has represented a significant threat to this unique ecosystem and its multiple functions. Understanding the extent, intensity and environmental impacts caused by fires in the Pantanal, is of unique importance for the preservation of the biome's biodiversity. Remote sensing techniques have played an important role in detecting and mapping burnt areas, especially SAR (Synthetic Aperture Radar) orbital systems, that are able to collect data in regions with frequent cloud cover or during extreme fire events. In this context, the objective of this study was to evaluate the potential of the U-Net semantic segmentation network applied to SAR data in the detection of burnt areas in the Brazilian Pantanal. For this, a semi-automatic annotated dataset was generated and considered as ground truth to evaluate the result obtained by the network. Two input datasets were evaluated in the detection of burnt areas, one containing optical and SAR data whereas the other containing only SAR data. The predictions of the two datasets were consistent with the semi-automatically generated annotation, showing similar spatial distribution but presenting a greater number of burnt areas. The model using both optical and SAR data achieved IoU (Intersection of Union) of 0.69 whereas the SAR only model had 0.60. Considering the amount of available data and the complexity of burnt area detection, the predictions achieved were adequate.

1. INTRODUCTION

The Pantanal biome is the largest and one of the most pristine wetlands in the world. The biome is internationally recognized for its ecological richness, covering a wide variety of habitats, such as wetlands, rivers, lakes, forests, savannahs, and grasslands (WWF, 2023). The Pantanal, which is located in the central region of South America (150,355 km^2), mainly in Brazil (about 140,000 km^2), also extending into Paraguay and Bolivia, is still responsible for providing a series of essential ecosystem services for local and national communities. Fishing, agriculture, and tourism are key economic activities for the Pantanal population (Alho et al., 2019).

The Pantanal plays a crucial role in the global ecological balance. Its biodiversity is essential for maintaining the health of the planet. This important wetland is home to remarkable biological diversity, including hundreds of species of birds, mammals, reptiles, and fish, where several of them are classified as threatened by the global red list (IUCN, 2023), such as the Jaguar (Panthera onca), Giant Anteater (Myrmecophaga tridactyla), Giant Otter (Pteronura brasiliensis) and Marsh Deer (Blastocerus dichotomus). The flora of the biome is also characterized by a wide variety of plants adapted to the specific conditions of this ecosystem with strong influence from neighbouring biomes: Amazonia, to the north, Cerrado, to the east, Atlantic Forest, center-south, and Chaco of Bolivia and Paraguay, to the west.

The biome works as a natural sponge, absorbing large amounts of water during heavy rains and gradually releasing it during periods of drought. This regulation of water flow is crucial for maintaining the balance of the rivers in the Pantanal watershed and for the maintenance of other adjacent ecosystems, such as the Amazon Forest.

In recent years, the Pantanal has faced major challenges and threats. Forest fires, deforestation, agricultural expansion, and climate change have negatively impacted this important ecosystem. Fires in the Pantanal cause significant damage to vegetation, directly affecting fauna and flora. Many endemic species depend on wetlands for their survival and reproduction, and habitat loss due to fires can lead to local extinction of these species. In addition, fires release large amounts of carbon dioxide into the atmosphere, intensifying the greenhouse effect and contributing to climate change.

In 2020, the Pantanal suffered one of the biggest wildfires in its history. A technical report by the Laboratory of Environmental Satellite Applications at the Federal University of Rio de Janeiro (LASA-UFRJ), showed that the fire affected more than 20% of its area until October, resulting in significant loss of habitats and the death of countless species (Libonati et al., 2020). The Brazilian program named Queimadas (Burned, in English), developed by the National Institute for Space Research (Instituto Nacional de Pesquisas Espaciais, INPE) for monitoring burned areas and active fire, estimated that approximately 40,606 km^2 was burnt in Brazilian Pantanal from January until October 2020 (INPE, 2020). Still according to the Queimadas program, in 2019 there was a 415% increase in hotspots compared to the average for the years 2010 to 2018 throughout Pantanal. The occurrence of fires continued at an accelerated pace, when the accumulated number of hotspots of 2020 increased by 223% in relation to

hotspots in 2019. Furthermore, among the 742,977 hotspots that occurred in the biome in 2020, almost 87 % were from July 20 to November 22.

In this context, the preservation of the Pantanal is essential to guarantee the maintenance of its ecosystem services, its biodiversity, and its fundamental role in regulating the water cycle. Therefore, monitoring burned areas in the biome is essential to understand their environmental impacts and implement appropriate management strategies. Remote sensing techniques allow obtaining accurate and updated data, which helps in understanding the extent, intensity, propagation patterns and assessment of the environmental impacts caused by forest fires. Optical remote sensing has played an important role in detecting and mapping burnt areas (Bright et al., 2019; Elhag et al. 2020; Delcourt et al., 2021). However, this data is subject to adverse weather conditions. Active sensors operating in the microwave spectrum, such as SAR (Synthetic Aperture Radar) orbital systems, are capable of acquiring data regardless of atmospheric conditions. This allows for reliable data acquisition in regions with frequent cloud cover or during extreme fire events (Tariq et al., 2021; Zhou et al., 2019; Mastro et al, 2022).

Coupled with the ability of the SAR systems of acquiring data regardless of illumination and atmospheric conditions, deep learning methods have shown great potential for extracting patterns of changes in images (Ban et al., 2020; Higa et al., 2022; Zhang et al., 2021), particularly semantic segmentation networks, such as the U-Net, proposed by Ronneberger et al. (2015). U-Net is a convolutional neural network architecture that performs semantic segmentation of images. The main feature of this network is its ability to learn to segment objects at different spatial scales, resulting in a more accurate segmentation of objects of interest.

The purpose of this study was therefore to evaluate the potential of the U-Net semantic segmentation model applied to SAR data in detecting burned areas in the Brazilian Pantanal. The model was validated by comparing it with semi-automatically generated annotation data from Sentinel-2 optical images.

2. METHODOLOGY

Sentinel-1 and 2 satellite optical and SAR data were used as input dataset. An annotated dataset was generated semi-automatically from the Sentinel-2 optical data; it was used in this study as ground truth. The annotation was also compared with the Kernel density map generated from hotspots that were acquired through the Queimadas program (INPE, 2020). Two datasets were defined for the application of the U-Net network for the detection of burned areas in the study area, one based on optical and SAR data and the other using only SAR data. The results were spatially and thematically compared with the generated annotation. The overall framework of the research is shown in Figure 1.

2.1 Study Area

The continuous and increasing degradation of the Pantanal biome due to fires, makes clear the need to preserve the ecological balance of the biome. Among the forms of conservation and preservation of biomes, the creation of Conservation Units (CUs) is fundamental for the protection of natural areas and consequent maintenance of ecological processes (Angelsen and Kaimawotiz, 2001). CUs are vital in responding to emerging challenges, such as water protection, disaster risk reduction and climate change. Therefore, the study area is partially inserted in a Brazilian Pantanal CU named Encontro das Águas State Park (EASP), Mato-Grosso State, as shown in Figure 2.

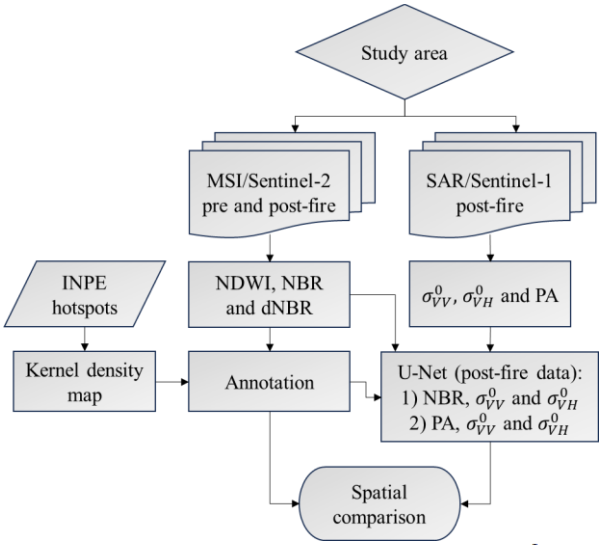

Figure 1. Overall flowchart of methodology, where σ^0_{VH} and σ^0_{VV} refers to the SAR backscatter coefficients, PA to the Polarization Averaging polarimetric index, NBR and NDWI to the Normalized Burn Ratio and Normalized Difference Water Index optical indices, respectively, and dNBR to the difference between pre- and post-fire NBRs.

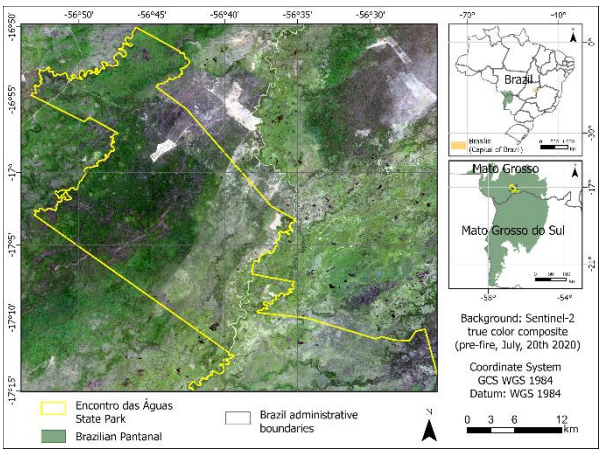

Figure 2. Location map of the study area.

The considered fire events for this study occurred in the period from July 20 to November 22, 2020. According to the data provided by the Queimadas program (INPE, 2020), during this period, the study area was severely affected by fire, with a total of 49,310 hotspots detected from satellites. The hotspots can be accessed from the program's database, available at the https://queimadas.dgi.inpe.br/queimadas/bdqueimadas portal, selecting the Export Data option, and configuring it for the country Brazil, mentioned period and Pantanal biome.

To show the extent of fire occurrence in the study area, a post-fire true color composite image (R(B4) G(B3) B(B2)) was generated from Sentinel-2 images acquired on November 22, 2020, as shown in Figure 3. Comparing with Figure 2, which shows the study area also in true color composite but before the burning period (images acquired on 20 July 2020), the extent of the vegetation area illustrated in Figure 3, decreases considerably, severely degrading the EASP CU.

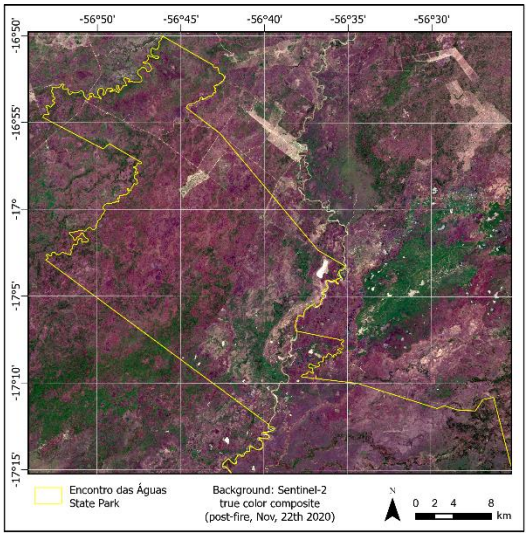

Figure 3. True color composite from the study area of Sentinel-2 images acquired on November 22, 2020 (post-fire), where the yellow polygon indicates the EASP CU. Purplish areas represent burnt areas.

2.2 Kernel density map generation

For a better understanding of the intensity of the hotspots throughout the study area, a Kernel density map was generated. From the Kernel map, it is possible to spatially analyze the areas most affected by fire and compare it with the annotation generated using Sentinel-2 optical data, verifying its consistency. For the generation of the Kernel density map, hotspots were acquired from the database of the Queimadas program (INPE, 2020). The period configured to obtain the hotspots was the intense burning period considered for this study, from July 20 to November 22, 2020.

2.3 Image Acquisition and Preprocessing

Sentinel-1 and 2 data were downloaded through their official repository, i.e., the European Space Agency (ESA) Copernicus Open Access Hub portal, available at https://scihub.copernicus.eu/ (exploiting the free, full, and open Copernicus License). Acquisition dates are as close as possible to the event dates that have been selected.

2.3.1 MSI/Sentinel-2: The Sentinel-2 optical images are acquired by the MultiSpectral Instrument (MSI) sensor and have 13 spectral bands, with three bands in the visible spectrum, Blue (492.4 nm), Green (559.8 nm) and Red (664.6 nm), and one in the Near InfraRed (NIR, 832.8 nm) with a spatial resolution of 10 meters; four bands in Red Edge (RE), RE-1 (704.1 nm), RE-2 (740.5 nm), RE-3 (782.8 nm) and RE-4 (864.7 nm) and two in Short Wave InfraRed (SWIR), SWIR-1 (1613.7) and SWIR-2 (2202.4), with a spatial resolution of 20 meters; and also 3 bands used in the atmospheric correction of the scene, with a resolution of 60 meters: Aerosol (442.7 nm), Water Vapor (945.1 nm) and Cirrus (1373.5 nm) (ESA, 2023).

For this study, pre- and post-event Sentinel-2 optical images calibrated in surface reflectance (Level 2, Bottom of Atmosphere, BOA) acquired respectively on July 20 and November 22, 2020, were selected. The images were resampled to 20 meters by nearest neighbor interpolation and the NBR (Normalized Burn Ratio) and NDWI (Normalized Difference Water Index) indices were calculated. Then, the difference (dNBR) between pre- and post-event NBRs was also calculated, which are used to assess the extent and severity of burned areas. Details in Table 1.

Acronym	Formulation	Reference
NDWI	$\frac{\rho_{Green} - \rho_{NIR}}{\rho_{Green} + \rho_{NIR}}$	Mcfeeters (1996)
NBR	$\frac{\rho_{NIR} - \rho_{SWIR1}}{\rho_{NIR} + \rho_{SWIR1}}$	Key and Benson (1999)
dNBR	$NBR_{pre} - NBR_{post}$	Key and Benson (2006)
PA	$\frac{\sigma^0_{VH} - \sigma^0_{VV}}{2}$	Dos Reis et al. (2019)

Table 1. Formulations of used spectral indices and difference. ρ_{Green}, ρ_{NIR}, and ρ_{SWIR1}, refer to reflectance in the green, Near InfraRed, and Short-Wave InfraRed-1 Sentinel-2 spectral bands, respectively.

2.3.2 SAR/Sentinel-1: Sentinel-1 satellites incorporate a SAR (Synthetic Aperture Radar) instrument that operates in the C band at a frequency of 5.404 GHz. The system has four distinct acquisition modes: SM (Stripmap Mode), IW (Interferometric Wide Swath Mode), EW (Extra-Wide Swath Mode) and WV (Wave Mode). IW is the main mode of land data acquisition and data is acquired over a 250 km swath with a spatial resolution of 5 m by 20 m. This mode acquires images in three sub swaths using the TOPSAR technique (Terrain Observation with Progressive Scans SAR). SAR images can still be provided in "complex" format, known as Single Look Complex (SLC), and Ground Range Detected (GRD), which consists of pre-processed SAR data projected to ground range (ESA, 2023).

SAR sensors have become an important tool to assist in the study and characterization of burnt areas, given their characteristics of independence from solar radiation, and low interference from clouds, smoke, and fog, rain among other meteorological conditions. SAR image processing various information about the target to be extracted, such as electrical components (dielectric constant/ water content), roughness and geometry (Jensen, 2009). These characteristics determine the intensity of backscattering and can become great allies in the characterization and monitoring of areas of natural vegetation affected by fire events.

For this study, GRD Sentinel-1 C-band SAR images, in IW mode and VV and VH polarizations, were selected. The SAR images were acquired only after the fire event, on November 24, 2020. These images were converted into the backscattering coefficients σ^0_{VV} and σ^0_{VH}, based on the following pre-processing steps: orbit correction; removal of thermal noise; data calibration; application of the Refined Lee filter with 3 × 3 window size; and terrain correction based on SRTM (Shuttle Radar Topography Mission) digital elevation model. In this last process, the spatial resolution of the images was also downsampled to 20 m to grant consistency with Sentinel-2 data. All the processing steps have been carried out in the ESA SNAP software After preprocessing, the polarimetric index Polarization Averaging (PA) was calculated (Table 1). To show the sensitivity of SAR data to burned areas, Figure 4 illustrates the (R)PA (G)VV (B)VH color composite, i.e., the Red channel is assigned to the PA polarimetric index, the Green channel to the backscatter coefficient σ^0_{VV} and the Blue channel to the backscatter coefficient σ^0_{VH}.

The red channel was attributed to the PA polarimetric index due to its response to burned areas with brighter pixels, as opposed to the σ^0_{VV} and σ^0_{VH} backscatter coefficients, which present darker

pixels. Therefore, the areas in red in Figure 4 indicate possibly burned areas.

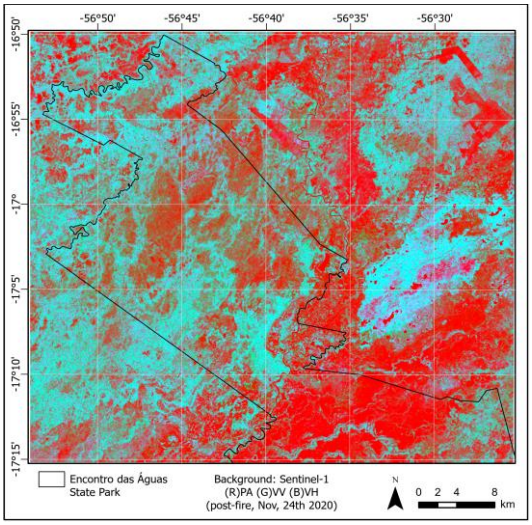

Figure 4. Color composite (R)PA (G)VV (B)VH from the study area of Sentinel-1 images acquired on November 24, 2020, where the black polygon indicates the EASP CU.

2.4 Semi-automatic annotation generation

The dNBR calculated from the pre- and post-fire NBR index, was used to semi-automatically generate the annotation for the application of the U-Net network. For this, a threshold was first applied to the dNBR to select only the severely burned areas, defined in the range of +0.66 to +1.30, by Key and Benson (2006) (Table 2) and confirmed by a qualitative visual inspection. This threshold was applied to isolate only severely burned areas from other burnt severity levels, thus allowing the U-Net semantic segmentation network model to learn from effectively burned areas avoiding false positives.

Severity level	dNBR range
Enhanced regrowth, high	–500 to –251
Enhanced regrowth, low	–250 to –101
Unburned	–100 to +99
Low severity	+100 to +269
Moderate-low severity	+270 to +439
Moderate-high severity	+440 to +659
High severity	+660 to +1300

Table 2. Ordinal severity levels and range of dNBR (scaled by 10^3), to the right.
Source: Key and Benson (2006)

In addition, a water mask was applied to remove water bodies since some of them presented dNBR values similar to burnt areas. The water mask was generated by applying a threshold to the optical-based NDWI index (Normalized Difference Water Index) defined by Mcfeeters (1996) as NDWI ≥ 0. Finally, the Sieve filter was applied to remove areas with less than 300 isolated pixels. The final product was a binary image, representing only burned and unburned areas.

The generated annotation was compared with the Kernel density map, which was created based on the hotspots acquired from the Queimadas program for the period considered for this study, to qualitatively verify its consistency. In addition, the annotation was used as ground truth to compare the results obtained through the application of the U-Net network.

2.5 U-net semantic segmentation network configuration and application

For application on the U-net network, two post-fire datasets were tested for comparison purposes. The first set was formed by Optical and SAR data, i.e., the NBR optical index and the σ^0_{VV} and σ^0_{VH} backscatter coefficients from the SAR images, while the second set contained only the SAR data σ^0_{VV}, σ^0_{VH} and the PA polarimetric index. Both datasets were stacked, forming two 3-bands products (2666 pixels by 2349 pixels), corresponding exactly to the same area of the generated annotation.

Due to the high memory requirement of the computer's GPU, images need to be divided into smaller patches for the training of the U-Net network. 256 pixels by 256 pixels patches were used. Since the dimension of the two datasets (Optical/SAR and only SAR) and the created annotation (2666 pixels x 2349 pixels) was not divisible by the size defined for the patches, they were cropped to the nearest size divisible by the patches size and from the top left corner, removing excess pixels and forming products measuring 2560 pixels by 2304 pixels. Thus, the data were divided into patches of 256 pixels by 256 pixels using the Patchify library and forming 90 complete patches (9 patches x 10 patches) for each product.

For the customization of the U-Net network, the Python segmentation-models library e was used. The patches were divided into a training (75%) and a validation dataset (25%) according to a consolidated training approach. The hyperparameters used are specified in Table 3. In addition, Data Augmentation was used to artificially increase the size of the dataset through 90° rotation; width and height shift and zoom were defined as 0.3, horizontal and vertical flips as True and the fill mode was set as reflection.

Hyperparameter	Specification
Encoder	ResNet-34
Optimizer	Adam
Epochs	100

Table 3. Hyperparameters used to customize the U-Net network.

After processing the U-Net network, figures representing the spatial distribution of the burnt areas referring to the prediction of the two sets of data (Optical/SAR and only SAR) were generated. The area represented as burnt was calculated for the two predictions, as well as for the generated annotation. The IoU (Intersection of Union) and the processing time for each dataset were also calculated. Finally, the processing generated the loss and accuracy curves for both the training and validation data.

3. RESULTS AND DISCUSSION

The Kernel density map indicating the intensity of hotspots acquired from the Queimadas program (INPE), throughout the study area from July 20 to November 22, 2020, is illustrated in Figure 5.

The Kernel density map (Figure 5) shows that the study area was severely affected by fire in the considered period, also indicating several areas of greater severity (stronger red). The annotation generated semi-automatically from optical data is presented in Figure 6, in which the pixels labeled as 1 (reddish pixels) refer to the burnt areas while the pixels labeled as 0 (white background) to the areas not affected by the fire.

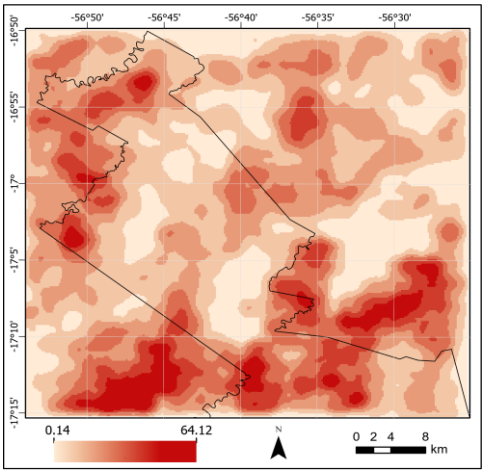

Figure 5. Kernel density map of hotspots derived from the Queimadas program (INPE) from July 20 to November 22, 2020, of the study area. The stronger the red, the greater the density of hotspots. The black polygon indicates the EASP CU.

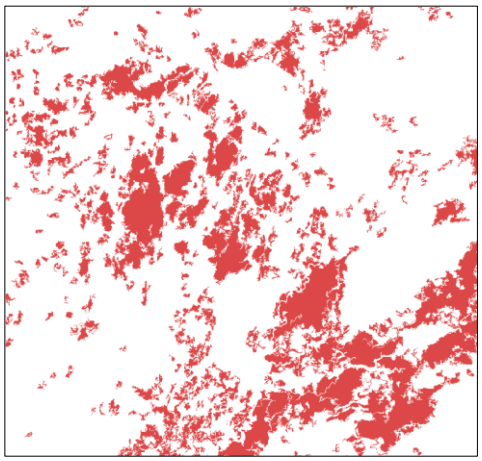

Figure 6. Annotation generated semi-automatically from the high burnt severity threshold, water mask and Sieve filter applied to the dNBR, that indicates the burnt areas in reddish pixels.

Comparing the Kernel density map (Figure 5) and the generated annotation (Figure 6), the two products showed a qualitative consistency in the spatial distribution of areas affected by fire, confirming the intensity of the event in the study area. This spatial distribution is also confirmed from the (R)PA (G)VV (B)VH color composite of the post-fire SAR images acquired on November 24, 2020, shown in Figure 4. It is also important to highlight that the SAR images are capable of not representing water bodies as burnt areas, which can be seen mainly in the lower part of the EASP in Figure 4. The opposite was seen in the dNBR optical product that was used to generate the annotation, as it was necessary to apply a mask for removing water bodies due to spectral similarity between targets.

Regarding the application of the U-Net network, Figure 7 a and b, respectively, illustrates the predictions of burnt areas referring to the optical/SAR (NBR, σ^0_{VV} and σ^0_{VH}) and SAR (σ^0_{VV}, σ^0_{VH} and PA) datasets.

The prediction of the two datasets presented in Figure 7, showed spatially similar results with the generated annotation (Figure 6), however, detecting a greater number of burnt areas in relation to the annotation (false positives). Despite the annotation used to train the U-Net network was generated only from a high burn severity threshold, the false positives can be attributed to the sensitivity of SAR images in detecting burned areas with a lower severity. Considering the defining characteristics, especially of the backscatter of the radar signal, such as water content and surface roughness, SAR images may present a more sensitive detection compared to optical images.

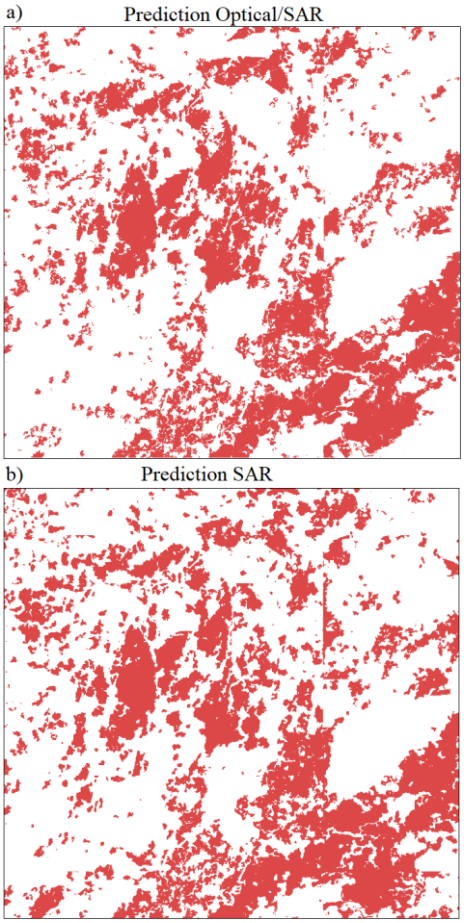

Figure 7. Predictions resulting from the application of the U-Net network to the (a) optical/SAR and (b) SAR datasets, where the reddish pixels indicate the burnt areas.

Comparing Figures 3 and 4, which show the response from optical and SAR data, in true color composite and (R)PA (G)VV (B)VH color composite, respectively, Figure 3 shows the burned areas scattered throughout the area. Figure 4, on the other hand, presents different characteristics, better defining the burned areas, due to the dominant mechanisms of the response of the radar signal after the fire. Zhou el al. (2019) explains that the dominant backscattering mechanism of vegetation before fire is volume scattering from the canopy layer of the vegetation. After a fire, as the vegetation is burned leaving part of the ground exposed, the dominant mechanism becomes surface scattering, which mainly depends on the roughness and moisture content of the soil. Furthermore, Mastro et al. (2022) and Tariq et al. (2021) state that the C-band backscatter coefficients are capable of detecting fire disturbances efficiently due to their sensitivity to changes in the structure of the vegetation affected by fire.

To reduce the number of false positives, an alternative could be to adjust the burn severity range applied to the dNBR, from which the annotation was generated, to an interval that comprises areas that were effectively burned, i.e., decrease the interval of burn severity level proposed by Key and Benson (2006). Thus, optical

data would possibly detect a smaller burned area to generate the annotation, enabling the network to learn from SAR data directly from very severely burned areas.

The processing of the U-Net network also generated the Loss (Jaccard loss function) and Accuracy curves resulting from the training and validation of the two sets of data (optical/SAR and only SAR data), shown in Figure 8.

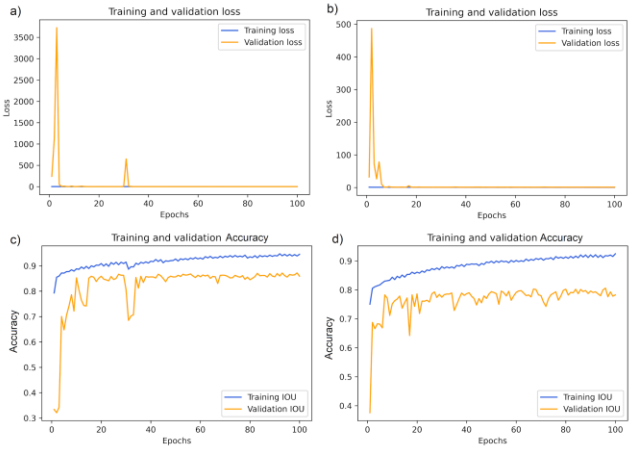

Figure 8. Loss (Jaccard loss function) and accuracy curves resulting from training and validation data for the optical/SAR dataset (a and c) and the SAR dataset (b and d).

The loss and accuracy curves show that the validation data of both datasets adjusted well to the model and the model's performance stabilizes after a few dozen epochs. In addition, both validation loss curves (orange curves in a and b) continuously converge to zero without much oscillation, which indicates a consistent result. The IoU measure and processing time for each dataset, in addition to the areas presented as burnt in the two datasets and the annotation, are presented in Table 4.

Data	Area labeled as burned area (ha)	IoU	Processing time *
Original Annotation	54,789.44	-	-
Optical/SAR	72,045.68	0.69	14′14″
SAR	79,200.20	0.60	14′12″

Table 4. Results obtained after processing the U-Net network in both datasets. * Desktop Workstation Specifications: Intel Core i9-12900K Processor (3.2GHz / 5.2GHz); RAM Memory of 64GB DDR4; Video Card Specification: Nvidia RTX A5000 24GB DDR6, 8192 CUDA CORE.

The dataset including optical and SAR images (NBR, σ^0_{VV} and σ^0_{VH}) presented higher performance with an IoU of 0.69. However, the dataset with only SAR data (σ^0_{VV}, σ^0_{VH} and PA) presented an IoU of 0.60. In addition, both datasets lead to similar results in terms of burnt areas with similar processing times, as detailed in Table 4. The data set with the best performance contains the NBR optical index, which was developed by the author in order to detect burned areas, and was also used to calculate the dNBR difference, which in turn was used to generate the annotation. Even so, the difference of the IoU compared to the dataset containing only SAR data was 0.09.

Considering the small data set involved in the detection of burnt areas applied in a deep learning approach, the level of accuracy achieved of the predictions were adequate. The result indicates consistency and potential in using only SAR data in detecting burned areas, compared to the use of optical data together with SAR data.

4. CONCLUSIONS

The Pantanal biome plays an essential role for Brazil and the world, providing vital ecosystem services, harboring unique biological diversity, and regulating hydrological and climate cycles. However, fires represent a serious threat to this valuable ecosystem, causing significant environmental and socioeconomic impacts. It is essential to adopt effective fire prevention and control measures and implement appropriate management strategies in areas affected by the fire to ensure the preservation of the Pantanal biome and its multiple functions.
This study showed a semi-automatic way of generating the annotation to be used in a deep learning approach, the U-Net semantic segmentation network, since this is a manual and time-consuming step. Additionally, two datasets (Optical/SAR and only SAR data) were evaluated in the detection of burnt areas using the U-Net. The predictions of the two datasets were consistent with the semi-automatically generated annotation, showing similar spatial distribution but presenting a greater number of burnt areas (Figure 7 and Table 4, respectively), i.e., false positives. However, this study indicates the potential of using SAR data in the detection of burnt areas in the absence of optical data, due to the characteristics that define its response, such as moisture content and surface roughness. The research also showed a promising result for a small data set that can be explored more intensively with larger datasets.

Further planned developments are to exploit the Rapid Mapping vector dataset produced by the Copernicus Emergency Management Service (CEMS) in case of Fire events as training dataset for the U-Net model. A portion of the same data not used in the training phase can be used to validate the trained model in different areas, to also evaluate the generalisation capabilities, in addition evaluate the use of different SAR features for the application in the U-Net network.

ACKNOWLEDGEMENTS

This study was financed in part by the Coordenação de Aperfeiçoamento de Pessoal de Nível Superior – Brasil (CAPES) - Finance Code 001, Grants: nº 88887.817766/2023-00 and nº 88887.817758/2023-00, and by São Paulo Research Foundation (FAPESP), Grant: nº 2021/06029-7.

REFERENCES

Alho, C. J. R.; Mamede, S. B.; Benites, M.; Andrade, B. S.; Sepúlveda, J. J. O., 2019. Threats to the biodiversity of the Brazilian Pantanal due to land use and occupation. Ambiente & Sociedade, 22. doi.org/10.1590/1809-4422asoc201701891vu2019L3AO.

Angelsen. A.; Kaimawotiz, D., 2001. Agricultural Technologies and Tropical Deforestation. Wallingford. UK: Biddles Ltd, Guildfor and King´s Lynn, p. 422.

Ban, Y.; Zhang, P.; Nascetti, A.; Bevington, A. R., Wulder, M. A., 2020. Near Real-Time Wildfire Progression Monitoring with Sentinel-1 SAR Time Series and Deep Learning. *Scientific Reports* 10, 1322. doi.org/10.1038/s41598-019-56967-x.

Bright, B. C.; Hudak, A. T.; Kennedy, R. E; Braaten, J. D.; Khalyani, A. H., 2019. Examining post-fire vegetation recovery with Landsat time series analysis in three western North American forest types. Fire Ecology, 15, 8. doi.org/10.1186/s42408-018-0021-9.

Delcourt, C. J. F.; Combee, A.; Izbicki, B.; Mack, M. C.; Maximov, T.; Petrov, R.; Rogers, B. M.; Scholten, R. C.; Shestakova, T.A.; Van Wees, D.; Veraverbeke, S., 2021. Evaluating the Differenced Normalized Burn Ratio for Assessing Fire Severity Using Sentinel-2 Imagery in Northeast Siberian Larch Forests. Remote Sensing, 13, 2311. doi.org/10.3390/rs13122311.

Dos Reis, A. A., Franklin, S. E., Mello, J. M., Acerbi Junior, F. W., 2019. Volume estimation in a Eucalyptus plantation using multi-source remote sensing and digital terrain data: A case study in Minas Gerais State, Brazil, *Int. J. Remote Sens.* 40(7), 2683-2702. doi.org/10.1080/01431161.2018.1530808.

Elhag, M.; Yimaz, N.; Bahrawi, J.; Boteva, S., 2020. Evaluation of Optical Remote Sensing Data in Burned Areas Mapping of Thasos Island, Greece. Earth Syst Environ 4, 813–826. doi.org/10.1007/s41748-020-00195-1.

ESA (The European Space Agency), 2023. Sentinel-2 MSI User Guide. sentinels.copernicus.eu/web/sentinel/user-guides (30 July 2023).

Higa, L.; Marcato Junior, J.; Rodrigues, T.; Zamboni, P.; Silva, R.; Almeida, L.; Liesenberg, V.; Roque, F.; Libonati, R.; Gonçalves, W.N.; et al., 2022. Active Fire Mapping on Brazilian Pantanal Based on Deep Learning and CBERS 04A Imagery. Remote Sens. 14(3), 688. doi.org/10.3390/rs14030688.

INPE. Portal do Monitoramento de Queimadas e Incêndios Florestais, 2020. queimadas.dgi.inpe.br/queimadas/bdqueimadas (20 June 2023).

IUCN (International Union for Conservation of Nature and Natural Resources), 2023. The IUCN Red List of Threatened Species. iucnredlist.org>. (30 June 2023).

Jensen, J. R., 2009. Remote Sensing of the Environment: An Earth Resource Perspective, 2nd Edition, Pearson Education India, New Delhi.

Key, C. H., Benson, N. C., 2006. Landscape Assessment (LA): Sampling and Analysis Methods. USDA Forest Service General Technical Report RMRS-GTR-164-CD.

Key, C. H., Benson, N. C., 1999. The Normalized Burn Ratio (NBR): A Landsat TM radiometric measure of burn severity. U.S. Dep. of the Interior, Northern Rocky Mountain Sc. Centre.

Libonati, R., Belém, L., Rodrigues, J. A., Lemos, F., Sena, C. A. P., Pinto, M. M., Carvalho, I. A., 2020. Nota técnica LASA - Área queimada Pantanal: situação até 18 de outubro 2020. Sistema ALARMES (Alerta de Área queimada com Monitoramento Estimado por Satélite). p. 12, Rio de Janeiro, Laboratório de Aplicações de Satélites Ambientais – UFRJ. doi.org/10.13140/RG.2.2.26367.02721.

Mastro, P.; Masiello, G.; Serio, C.; Pepe, A., 2022. Change Detection Techniques with Synthetic Aperture Radar Images: Experiments with Random Forests and Sentinel-1 Observations. Remote Sens. 2022, 14, 3323. doi.org/10.3390/rs14143323.

Mcfeeters, S. K., 1996. The use of the Normalized Difference Water Index (NDWI) in the delineation of open water features. *Int. J. Remote Sens.*, 17(7), 1425-1432. doi.org/10.1080/01431169608948714.

Ronneberger, O., Fischer, P., Brox, T., 2015. U-Net: Convolutional Networks for Biomedical Image Segmentation. International Conference on Medical Image Computing and Computer-Assisted Intervention (MICCAI-2015), Springer, LNCS, 9351, 234-241. doi.org/10.1007/978-3-319-24574-4_28.

Tariq, A.; Shu, H.; LI, Q.; Altan, O.; Khan, M. R.; Baqa, M. F.; LU, L., 2021. Quantitative Analysis of Forest Fires in Southeastern Australia Using SAR Data. Remote Sensing, 13, 2386. doi.org/10.3390/rs13122386.

Zhang, Q., Ge, L., Zhang, R., Metternicht, G.I., Liu, C., Du, Z., 2021. Towards a Deep-Learning-Based Framework of Sentinel-2 Imagery for Automated Active Fire Detection. *Remote Sens.* 13(23), 4790. doi.org/10.3390/rs13234790.

Zhou, Z.; Liu, L.; Jiang, L.; Feng, W.; Samsonov, S.V., 2019. Using Long-Term SAR Backscatter Data to Monitor Post-Fire Vegetation Recovery in Tundra Environment. Remote Sensing, 11, 2230. doi.org/10.3390/rs11192230.

WWF (World Wildlife Fund), 2023. 5 interesting facts about the Pantanal, the world's largest tropical wetland. worldwildlife.org (20 June 2023).